Journal of KONBiN 2022
Volume 52, Issue 3
DOI 10.2478/jok-2022-0036

Adam CZABAN, Andrzej MISZCZAK
Gdynia Maritime University (Uniwersytet Morski w Gdyni)

INFLUENCE OF PRESSURE CHANGES ON THE VISCOSITY OF LUBRICATING OIL IN CFD SIMULATIONS OF CONICAL BEARING HYDRODYNAMIC LUBRICATION

Wpływ zmian ciśnienia na lepkość oleju smarnego w modelowaniu hydrodynamicznego smarowania stożkowego łożyska ślizgowego

Abstract: *The aim of this study is to consider the effect of pressure on the viscosity of lubricating oil in the adopted model of hydrodynamic lubrication and on the calculated flow parameters and operating parameters of a conical slide bearing. The numerical analysis consisted in solving the Reynolds type equation for the process of stationary hydrodynamic lubrication.*

Keywords: hydrodynamic lubrication, sliding bearing, conical bearing, viscosity, hydrodynamic pressure

Streszczenie: *Celem niniejszej pracy jest zbadanie, w jakim stopniu uwzględnienie wpływu ciśnienia na lepkość oleju smarnego, w przyjętym modelu hydrodynamicznego smarowania, oddziałuje na obliczane parametry przepływowe i eksploatacyjne analizowanego stożkowego łożyska ślizgowego. W badaniach wykorzystano znane z literatury równanie typu Reynoldsa, określające proces stacjonarnego hydrodynamicznego smarowania.*

Słowa kluczowe: hydrodynamiczne smarowanie, łożysko ślizgowe, łożysko stożkowe, lepkość, ciśnienie hydrodynamiczne

1. Introduction

This paper is a part of the authors' research on the hydrodynamic lubrication theory of slide bearings. The aim of this study is to consider the effect of pressure on the viscosity of lubricating oil in the adopted model of hydrodynamic lubrication and on the calculated flow parameters and operating parameters of a conical slide bearing.

The geometry of the conical slide bearing enables the simultaneous transfer of loads in the axial direction and in the direction perpendicular to the axis of rotation of the shaft. However, the non-classical geometry makes the equations of the hydrodynamic lubrication theory a bit more complicated than in the case of a journal bearings. These equations include terms resulting from the action of centrifugal forces. The model presented in this paper has already been used in the article [2], concerning the study of the effect of dimensionless heat flux on the inner surface of the shell. A similar model was used in the work [1], which concerned the hydrodynamic lubrication of a conical slide bearing with ferro-oil, which was under the influence of a external magnetic field.

In order to take into account the influence of pressure on bearing lubricating oil viscosity, the experimental data presented in the paper [4] was used. In papers [1] and [2], the experimental data were fitted with the curves described by appropriate models, which determine the effect of temperature, shear rate and pressure on the viscosity of the lubricating oil, and hence, on the calculated values of the flow and operating parameters of the conical slide bearings. In this work, the appropriate model coefficients were used on the basis of [1] and [2]. The obtained values were compared, i.e. those when the influence of pressure on the viscosity of the lubricating oil was taken into account, with the results when the viscosity of the lubricating oil was independent of the pressure. The model uses the Reynolds type equation in the dimensionless form and all calculated values are also dimensionless. The flow and operating parameters, obtained in simulations and compared, are as follows:

- dimensionless hydrodynamic pressure distributions,
- axial and radial load carrying capacities,
- friction forces,
- coefficients of friction.

This study gives important information on whether and when the influence of pressure on lubricating oil viscosity should be taken into account when designing conical slide bearings, which can significantly affect their reliability.

2. Bearing model

In Fig. 1 is shown the geometry of the investigated slide conical bearing. The equations of the mathematical model were written in the conical coordinate system [1, 2].

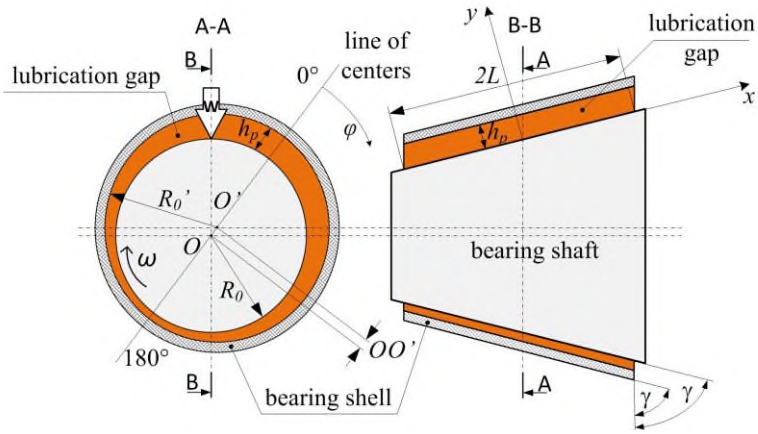

Fig. 1. The geometry of concerned slide conical bearing – radial and axial cross-section

The designations are as follows:

- $\varphi[^\circ]$ – circumferential coordinate, where: $0^\circ \le \varphi < 360^\circ$,
- $y[\mathrm{m}]$ – radial coordinate of the conical coordinate system,
- $x[\mathrm{m}]$ – longitudinal coordinate of the conical coordinate system,
- $R_0[\mathrm{m}]$ – journal radius at half length of the bearing,
- $R_0^{'}[\mathrm{m}]$ – inner radius of the shell at half length of the bearing,
- $\varepsilon_s[\mathrm{m}] = R_0^{'} - R_0$ – the radial clearance,
- $\gamma[^\circ]$ – the angle, which define the conical bearing geometry (for journal bearings $\gamma = 90^\circ$),
- $L[\mathrm{m}]$ – half the length of the conical bearing, measured in the longitudinal direction $x[\mathrm{m}]$,
- $OO'[\mathrm{m}]$ – bearing eccentricity,
- $h_p[\mathrm{m}]$ – lubrication gap height of the bearing, measured in the direction of the thickness of the lubricating layer, i.e. in the transverse direction $y[\mathrm{m}]$,
- $\omega[\mathrm{rad/s}]$ – angular velocity of the bearing shaft.
- $\mathbf{W}[\mathrm{N}]$ – load supported by the bearing.

In this research, the bearing with a full wrap angle was investigated. The following assumptions and conditions were adopted in the bearing model:

- the bearing operates in steady state,
- the bearing surfaces are smooth, rigid, without deformations,
- the axis of shaft rotation is parallel to the shell axis,
- the hydrodynamic pressure is generated due to the rotation of the bearing shaft with constant speed $\omega[\mathrm{rad/s}]$,

- the bearing shell is stationary,
- the bearing shaft carries a constant load,
- vibrations are neglected,
- the incompressible flow of non-Newtonian oil is laminar and non-isothermal,
- the pressure at the lubrication gap boundaries is equal to atmospheric pressure, while the end of the lubricating wedge in the circumferential direction is determined by the Reynolds [1, 2, 3, 5, 7, 8] (Swift – Steiber) boundary condition:

$$\left.\frac{\partial p}{\partial \varphi}\right|_{\varphi=\varphi_k} = 0, \tag{1}$$

- at the bearing shaft and shell surfaces, the components of the velocity of the oil layer have the same value as the surface to which they adhere,
- the temperature at the bearing shaft surface is constant, while the temperature at the shell inner surface is unknown.

The hydrodynamic pressure distribution in the lubrication gap was calculated by the solution of the dimensionless Reynolds type equation [1, 2], which can be written in the conical coordinate system as:

$$\begin{gathered}\Theta \frac{\partial}{\partial \varphi}\left(\int_0^{h_{p1}} \Gamma_m \mathrm{d}y_1 - h_{p1}\right) = \\ = \left(\frac{1}{\Theta}\frac{\partial^2 p_1}{\partial \varphi^2} + \frac{\cos\gamma}{L_1}\frac{\partial p_1}{\partial x_1} + \frac{\Theta}{L_1{}^2}\frac{\partial^2 p_1}{\partial x_1{}^2}\right)\int_0^{h_{p1}} \Gamma_d \mathrm{d}y_1 - \frac{\rho_1 \mathrm{Re}\psi\cos\gamma}{L_1}\frac{\partial}{\partial x_1}\left(\int_0^{h_{p1}} \Gamma_c \mathrm{d}y_1\right),\end{gathered} \tag{2}$$

where:

- $\psi = \frac{\varepsilon_s}{R_0} \sim 10^{-3}$ – the relative radial clearance,
- $\lambda = \frac{OO'}{\varepsilon_s}$ – the bearing relative eccentricity,
- $h_{p1} = \frac{h_p}{\varepsilon_s}$ – the dimensionless lubrication gap height, defined as:

$$h_{p1}(\varphi) = \frac{1+\lambda\cos\varphi}{\sin\gamma}, \tag{3}$$

- $y_1 = \frac{y}{\varepsilon_s}$ – the dimensionless coordinate in the direction of the layer thickness, where $0 \le y_1 \le h_{p1}$,

- $x_1 = \frac{x}{L}$ – the dimensionless coordinate in the longitudinal direction,
  where $-1 \le x_1 \le 1$,
- $L_1 = \frac{L}{R_0}$ – the dimensionless bearing length,
- $\Theta = 1 + L_1 x_1 \cos\gamma$ – the dimensionless (simplified) form of the Lame's coefficient of conical coordinate system,
- $p_1 = \frac{p}{p_0}$ – the dimensionless pressure, where $p\,[\mathrm{Pa}]$ is a absolute pressure, while

$$p_0 = \frac{U_0 \eta_0}{R_0 \psi^2}, \tag{4}$$

- $U_0[\mathrm{m/s}] = \omega R_0$ – the velocity value of shaft surface at half of its length,
- $\eta_0[\mathrm{Pa \cdot s}]$ – the characteristic value of dynamic viscosity,
- $\mathrm{Re} = \frac{\varepsilon_s U_0 \rho_0}{\eta_0}$ – the Reynolds number,
- $\rho_0[\mathrm{kg/m^3}]$ – the characteristic value of lubricating oil density.

The Eq. (2) also introduces the functions: $\Gamma_m(\varphi, y_1, x_1)$, $\Gamma_d(\varphi, y_1, x_1)$, $\Gamma_c(\varphi, y_1, x_1)$, where [1, 2]:

$$\int_0^{h_{p1}} \Gamma_m \,\mathrm{d}y_1 = \frac{\int_0^{h_{p1}} \int_0^{y_1} \frac{1}{\eta_1} \mathrm{d}y_1 \mathrm{d}y_1}{\int_0^{h_{p1}} \frac{1}{\eta_1} \mathrm{d}y_1}, \tag{5}$$

$$\int_0^{h_{p1}} \Gamma_d \,\mathrm{d}y_1 = \int_0^{h_{p1}} \int_0^{y_1} \frac{y_1}{\eta_1} \mathrm{d}y_1 \mathrm{d}y_1 - \left(\int_0^{h_{p1}} \Gamma_m \,\mathrm{d}y_1 \right) \left(\int_0^{h_{p1}} \frac{y_1}{\eta_1} \mathrm{d}y_1 \right), \tag{6}$$

$$\int_0^{h_{p1}} \Gamma_c \,\mathrm{d}y_1 = \left(\frac{1}{\Theta} \frac{\partial p_1}{\partial \varphi} \right)^2 \int_0^{h_{p1}} \Gamma_1 \,\mathrm{d}y_1 - 2 \frac{\partial p_1}{\partial \varphi} \int_0^{h_{p1}} \Gamma_2 \,\mathrm{d}y_1 + \Theta^2 \int_0^{h_{p1}} \Gamma_3 \,\mathrm{d}y_1, \tag{7}$$

while the integrals of functions $\Gamma_1(\varphi, y_1, x_1)$, $\Gamma_2(\varphi, y_1, x_1)$, $\Gamma_3(\varphi, y_1, x_1)$ are, as follows [1, 2]:

$$\int_0^{h_{p1}} \Gamma_1 \, \mathrm{d}y_1 = \int_0^{h_{p1}} \left[\int_0^{y_1} \left(\frac{1}{\eta_1} \int_0^{y_1} \Gamma_d^{\,2} \, \mathrm{d}y_1 \right) \mathrm{d}y_1 \right] \mathrm{d}y_1 - \left(\int_0^{h_{p1}} \Gamma_m \, \mathrm{d}y_1 \right) \left[\int_0^{h_{p1}} \left(\frac{1}{\eta_1} \int_0^{y_1} \Gamma_d^{\,2} \, \mathrm{d}y_1 \right) \mathrm{d}y_1 \right], \quad (8)$$

$$\begin{aligned} \int_0^{h_{p1}} \Gamma_2 \, \mathrm{d}y_1 = & \int_0^{h_{p1}} \left[\int_0^{y_1} \left(\frac{1}{\eta_1} \int_0^{y_1} (1-\Gamma_m)\Gamma_d \, \mathrm{d}y_1 \right) \mathrm{d}y_1 \right] \mathrm{d}y_1 + \\ & - \left(\int_0^{h_{p1}} \Gamma_m \, \mathrm{d}y_1 \right) \left[\int_0^{h_{p1}} \left(\frac{1}{\eta_1} \int_0^{y_1} \int_0^{y_1} (1-\Gamma_m)\Gamma_d \, \mathrm{d}y_1 \right) \mathrm{d}y_1 \right], \end{aligned} \quad (9)$$

$$\begin{aligned} \int_0^{h_{p1}} \Gamma_3 \, \mathrm{d}y_1 = & \int_0^{h_{p1}} \left[\int_0^{y_1} \left(\frac{1}{\eta_1} \int_0^{y_1} (1-\Gamma_m)^2 \, \mathrm{d}y_1 \right) \mathrm{d}y_1 \right] \mathrm{d}y_1 + \\ & - \left(\int_0^{h_{p1}} \Gamma_m \, \mathrm{d}y_1 \right) \left[\int_0^{h_{p1}} \left(\frac{1}{\eta_1} \int_0^{y_1} \int_0^{y_1} (1-\Gamma_m)^2 \mathrm{d}y_1 \right) \mathrm{d}y_1 \right]. \end{aligned} \quad (10)$$

The dimensionless oil viscosity $\eta_1[1]$, present in the above equations, is defined as:

$$\eta_1 = \frac{\eta_p}{\eta_0}, \quad (11)$$

where $\eta_p[\mathrm{Pa \cdot s}]$ is the oil apparent viscosity, generally dependent on temperature, shear rate and pressure, hence the dimensionless viscosity values were calculated with the following equation [1, 2]:

$$\eta_1(\varphi, y_1, x_1) = \eta_{1T}(\varphi, y_1, x_1) \cdot \eta_{1\dot{\gamma}}(\varphi, y_1, x_1) \cdot \eta_{1p}(\varphi, x_1). \quad (12)$$

The factor

$$\eta_{1T}(\varphi, y_1, x_1) = \exp\left(-\delta_T \mathrm{Br} T_0 T_1\right) \quad (13)$$

describes the changes in dimensionless viscosity depending on the dimensionless temperature $T_1[1]$:

$$T_1 = \frac{T - T_0}{T_0 \,\mathrm{Br}} \quad , \tag{14}$$

where T[K] is dimensional temperature, T_0[K] is the reference temperature, while the Brinkman number [1,2,8]:

$$\mathrm{Br} = \frac{{U_0}^2 \eta_0}{\kappa_0 T_0} \tag{15}$$

and $\kappa_0[\mathrm{W/(m \cdot K)}]$ is a characteristic value of lubricating oil thermal conductivity. The parameter $\delta_T\,[\mathrm{K}^{-1}]$ was obtained by fitting the curve described by Eq. (13) to the experimental data [1, 2, 4].

The three-dimensional distributions of the dimensionless temperature $T_1[1]$ in the conical slide bearing lubrication gap, were calculated in accordance with the following analytical solution of the energy equation [1, 2, 10]:

$$\begin{aligned} T_1(\varphi, y_1, x_1) = &-\frac{1}{\kappa_1}\int_0^{y_1}\left(\int_0^{y_1}\Lambda_1 \,\mathrm{d}y_1\right)\mathrm{d}y_1 - \frac{\cos^2\gamma}{\Theta^2\kappa_1}{\rho_1}^2{L_1}^2\,\mathrm{Re}^2\,\psi^2\int_0^{y_1}\left(\int_0^{y_1}\Lambda_2\,\mathrm{d}y_1\right)\mathrm{d}y_1 \\ &+\frac{2\cos\gamma}{\Theta\kappa_1}\rho_1 L_1\,\mathrm{Re}\psi\int_0^{y_1}\left(\int_0^{y_1}\Lambda_3\,\mathrm{d}y_1\right)\mathrm{d}y_1 - \frac{q_{c1}y_1}{\kappa_1} + 1 \end{aligned} \quad , \tag{16}$$

where the dimensionless thermal conductivity: $\kappa_1 = \kappa / \kappa_0$ ($\kappa[\mathrm{W/(m \cdot K)}]$ is the thermal conductivity of lubricating oil) and the dimensionless heat flux is defined as:

$$q_{c1} = -\kappa_1 \left.\frac{\partial T_1}{\partial y_1}\right|_{y_1 = 0} \quad . \tag{17}$$

The paper [2] shows the influence of the value of heat flux, which is exchanged between the oil in the lubrication gap and the inner surface of the shell, on the results obtained with this model. In these considerations it has been assumed that $q_{c1} = 0$.

In Eq. (16), the following designations were introduced [1, 2, 10]:

$$\Lambda_1(\varphi, y_1, x_1) = \eta_1\left(\frac{1}{\Theta}\frac{\partial p_1}{\partial \varphi}\frac{\partial \Gamma_d}{\partial y_1} - \Theta\frac{\partial \Gamma_m}{\partial y_1}\right)^2 + \frac{\eta_1}{{L_1}^2}\left(\frac{\partial p_1}{\partial x_1}\frac{\partial \Gamma_d}{\partial y_1}\right)^2, \tag{18}$$

$$\Lambda_2(\varphi, y_1, x_1) = \eta_1 \left[\left(\frac{1}{\Theta} \frac{\partial p_1}{\partial \varphi} \right)^2 \frac{\partial \Gamma_1}{\partial y_1} + 2 \frac{\partial p_1}{\partial \varphi} \frac{\partial \Gamma_2}{\partial y_1} + \Theta^2 \frac{\partial \Gamma_3}{\partial y_1} \right]^2, \tag{19}$$

$$\Lambda_3(\varphi, y_1, x_1) = \eta_1 \frac{\partial p_1}{\partial x_1} \frac{\partial \Gamma_d}{\partial y_1} \left[\left(\frac{1}{\Theta} \frac{\partial p_1}{\partial \varphi} \right)^2 \frac{\partial \Gamma_1}{\partial y_1} + 2 \frac{\partial p_1}{\partial \varphi} \frac{\partial \Gamma_2}{\partial y_1} + \Theta^2 \frac{\partial \Gamma_3}{\partial y_1} \right]. \tag{20}$$

The factor $\eta_{1\dot{\gamma}}(\varphi, y_1, x_1)$ in Eq. (12) describes the effect of shear rate on dimensionless viscosity of generalized non-Newtonian oil [1, 2, 8, 9]. The changes in the viscosity of the lubricating oil were assumed to be consistent with the Cross model, therefore:

$$\eta_{1\dot{\gamma}}(\varphi, y_1, x_1) = \frac{\eta_{1zero}}{1 + \left(k_{\dot{\gamma}}\, \dot{\gamma}\right)^{n_{\dot{\gamma}}}}, \tag{21}$$

where $\eta_{1zero}[1]$ is the dimensionless viscosity for low shear rates, i.e. when $\dot{\gamma} \to 0\,\mathrm{s}^{-1}$, while $k_{\dot{\gamma}}[\mathrm{s}]$ and $n_{\dot{\gamma}}[1]$ are experimental factors, obtained by fitting the curve described by Eq. (21) to the experimental data [1, 2, 4].

The shear rate was calculated according to the following relationship [1, 2]:

$$\dot{\gamma}(\varphi, y_1, x_1) = \sqrt{\frac{1}{2} \sum_{i=1}^{3} \sum_{j=1}^{3} \dot{\gamma}_{ij} \dot{\gamma}_{ji}}\ , \tag{22}$$

where $\dot{\gamma}_{ij}[\mathrm{s}^{-1}]$ are the components of the strain tensor [1, 2, 8]:

$$\mathbf{A}_1 = \mathbf{L} + \mathbf{L}^{\mathbf{T}}, \tag{23}$$

for which:

$$\mathbf{L} = \mathrm{grad}\, \vec{v}, \tag{24}$$

where

$$\vec{v} = \hat{\mathrm{i}} \cdot v_{\varphi} + \hat{\mathrm{j}} \cdot v_{y1} + \hat{\mathrm{k}} \cdot v_{x1} \tag{25}$$

is the lubricating oil velocity vector.

The dimensionless component in the peripheral direction:

$$v_1 = \frac{v_\varphi}{U_0} \tag{26}$$

and the dimensionless velocity component in the longitudinal direction:

$$v_3 = \frac{v_x L_1}{U_0}, \tag{27}$$

were calculated in accordance with the analytical solutions of momentum conservation equations [1, 10] (the transverse velocity component v_2 was neglected):

$$v_1(\varphi, y_1, x_1) = \frac{1}{\Theta}\frac{\partial p_1}{\partial \varphi}\Gamma_d - \Theta(\Gamma_m - 1), \tag{28}$$

$$v_3(\varphi, y_1, x_1) = \frac{1}{\Theta}\frac{\partial p_1}{\partial x_1}\Gamma_d - \rho_1 L_1 \mathrm{Re}\psi \frac{\cos\gamma}{\Theta}\Gamma_c. \tag{29}$$

The factor $\eta_{1p}(\varphi, x_1)$ in Eq. (12) determines the effect of pressure on the dimensionless viscosity. Due to the simplifications adopted for the thin lubricating layer, the model omits changes in pressure towards the height of the lubrication gap. It was assumed, that the viscosity depends on the pressure according to the following relationship [1, 2]:

$$\eta_{1p}(\varphi, x_1) = \ln(e + \delta_p p_0 p_1), \tag{30}$$

where $e \approx 2.718$ is the Euler's number and $\delta_p [\mathrm{Pa}^{-1}]$ is an experimental factor, obtained by fitting the curve described by Eq. (30) to the experimental data [1, 2, 4].

In order to determine whether it is important to consider the influence of pressure on the viscosity of the lubricating oil in the modelling of hydrodynamic lubrication of the conical slide bearing, the results obtained using the Eq. (12) and Eq. (30), were compared with the values obtained, when this effect was neglected, i.e. the equation has a constant value:

$$\eta_{1p}(\varphi, x_1) = 1. \tag{31}$$

The coefficients in Eq. (13), Eq. (21) and Eq. (30) were determined in papers [1, 2] by fitting the curves described by these equations to the experimental data obtained for 2% ferro-oil, which is not affected by the magnetic field. These results are presented in the paper [4]. The fitting of the curves described with these models was made using the least squares approximation method and the *lsqcurvefit* package from the Matlab software [1, 2]. The determined values, are:

- $Q_{\mathrm{Br}} = \delta_T \mathrm{Br} T = 3.4224[1]$,
- $Q_{\mathrm{p}} = \delta_T p_o = 2.7097[1]$,
- $\eta_{1zero} = 2.71[1]$,
- $k_{\dot{\gamma}} = 0.7129[\mathrm{s}]$ and $n_{\dot{\gamma}} = 0.1064[1]$,

for the following reference values:

- $T_0 = 363.0[\mathrm{K}]$
- $\eta_0 = 0.0263[\mathrm{Pa \cdot s}]$.

Furthermore, it was assumed, that:

- $\rho_0 = 950$ [kg/m^3] and $\rho_1 = 1[1]$,
- $\kappa_0 = 0.15[\mathrm{W/(m \cdot K)}]$,
- $\kappa_1 = 1[1]$,
- the dimensionless constant temperature at bearing shaft surface: $T_{1c} = 1$.

The mesh used in the calculationshad the following dimensions:

- 100 elements in the wrap angle direction,
- 50 elements in the bearing length direction,
- 10 elements in the bearing lubrication gap height direction.

The iterative Newton's method [1, 2, 6] has been implemented in order to determine the pressure distribution in the lubricating gap of the considered bearing. The first and second derivatives and mixed derivatives were approximated by finite differences. In the first step, the initial pressure distribution was calculated by omitting the nonlinear part in Eq. (2) and for the Gümbel (half-Sommerfeld) condition [1, 2, 7, 8], i.e. when $\varphi_k = 180^\circ$. In the next step the Eq. (30) was used to calculate the viscosity changes caused by pressure changes. The determined pressure distribution was then used to calculate the temperature distribution with the Eq. (16). In the next step, the influence of temperature on viscosity was considered by using the Eq. (13) and Eq. (12). Afterwards, the velocity components were calculated with the Eq. (28) and Eq. (29). The determined values of the velocity components were used for the calculation of the shear rate distribution, by using the Eq. (22). Then, the effect of shear rate on viscosity was taken into account with the Eq. (21). The updated viscosity values were used to determine the pressure corrections by solution of the Eq. (2) with the iterative Newton's method, and the improved pressure distribution was determined. This procedure was repeated until the condition for convergence and residuum was reached, i.e. when both values are less than 10^{-3}. Then it was checked if the Reynold’s condition was met. If not, then the φ_k value of the angle determining the end of the lubricating wedge location, was increased by $\Delta\varphi_k = 1^\circ$. After determining the φ_k, the final pressure distribution was calculated under the condition, that convergence and residuum: $<10^{-6}$.

The obtained final pressure distribution was used to calculate the transverse $C_{1T}[1]$ (perpendicular to the axis of shaft rotation) and the longitudinal $C_{1L}[1]$ (parallel to the axis of shaft rotation) dimensionless component of the bearing load carrying capacity, with the following relations [1, 10]:

$$C_{1T} = \sqrt{\left(\int_{-1}^{1}\int_{0}^{\varphi_k} p_1 \Theta \cos\varphi \sin\gamma \, d\varphi dx_1\right)^2 + \left(\int_{-1}^{1}\int_{0}^{\varphi_k} p_1 \Theta \sin\varphi \sin\gamma \, d\varphi dx_1\right)^2}, \tag{32}$$

$$C_{1L} = \sqrt{\left(\int_{-1}^{1}\int_{0}^{\varphi_k} p_1 \Theta \cos\varphi \cos\gamma \, d\varphi dx_1\right)^2 + \left(\int_{-1}^{1}\int_{0}^{\varphi_k} p_1 \Theta \sin\varphi \cos\gamma \, d\varphi dx_1\right)^2}. \tag{33}$$

The dimensionless friction force $Fr_1[1]$ was calculated with the following equation [1]:

$$Fr_1 = \sqrt{\left(\int_{-1}^{1}\int_{0}^{2\pi} \eta_1 \Theta \left.\frac{\partial v_1}{\partial y_1}\right|_{y_1=h_{p1}} d\varphi dx_1\right)^2 + \left(\int_{-1}^{1}\int_{0}^{2\pi} \eta_1 \Theta \left.\frac{\partial v_3}{\partial y_1}\right|_{y_1=h_{p1}} d\varphi dx_1\right)^2} \tag{34}$$

and the coefficient of friction $\mu_r[1]$ can be calculated as [1, 2, 8]:

$$\mu_r = \frac{\sqrt{C_{1T}{}^2 + C_{1L}{}^2}}{Fr_1}. \tag{35}$$

The simulations were carried out for the bearing with $\psi = 10^{-3}[1]$, for the dimensionless bearing lengths: $L_1 = 0.5$, $L_1 = 1.0$, $L_1 = 1.5$, at relative eccentricities: $\lambda = 0.1 - 0.9$, every 0.1.

3. Results

The simulation results were compared for the case, when the model takes into account the effect of dimensionless pressure on dimensionless viscosity, by substituting the Eq. (30) to Eq. (12), with the calculation results, for which the effect of dimensionless pressure on lubricating oil dimensionless viscosity is neglected, i.e. when in the Eq. (12), the Eq. (31)

is substituted. The results for the case, where the pressure effect was included, are marked in the charts legend as: $\eta(T_1, \dot{\gamma}, p_1)$, while the results for the case where the influence of pressure on viscosity of the lubricating oil were neglected, were marked as: $\eta(T_1, \dot{\gamma})$.

In Fig. 2 is shown the comparison of dimensionless pressure distributions in the lubricating gap: a) in the cross section, and b) in the longitudinal section, at the point of maximum dimensionless pressure p_{1max}, for a bearing with dimensionless length $L_1 = 0.5$ and the lowest tested value of relative eccentricity $\lambda = 0.1$.

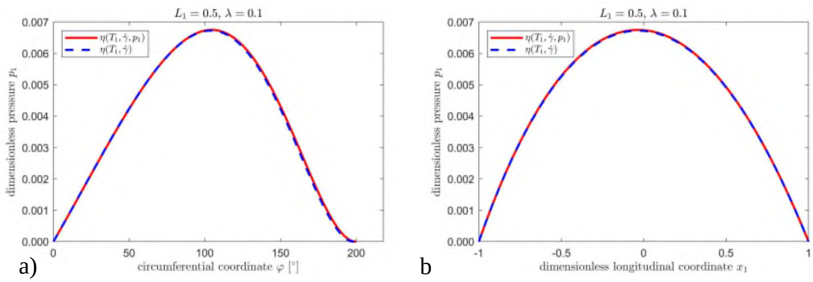

Fig. 2. The comparison of dimensionless pressure distributions p_1 in the lubricating gap: a) cross section, b) longitudinal section, at the point of maximum dimensionless pressure p_{1max}, for a bearing with dimensionless length $L_1 = 0.5$ and the relative eccentricity $\lambda = 0.1$

The changes in the obtained values of dimensionless pressure in the lubricating gap in this case are irrelevant. The situation becomes quite different as the value of the relative eccentricity increases. In Fig. 3 is shown the comparison of dimensionless pressure distributions in the lubricating gap: a) in the cross section, and b) in the longitudinal section, at the point of maximum dimensionless pressure p_{1max}, for a bearing with dimensionless length $L_1 = 0.5$ and the relative eccentricity $\lambda = 0.5$.

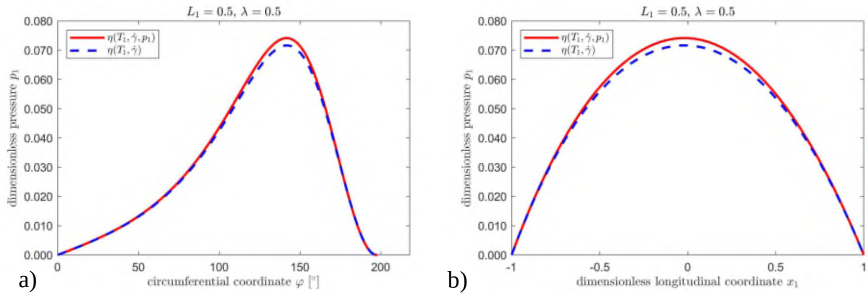

Fig. 3. The comparison of dimensionless pressure distributions p_1 in the lubricating gap: a) cross section, b) longitudinal section, at the point of maximum dimensionless pressure p_{1max}, for a bearing with dimensionless length $L_1 = 0.5$ and the relative eccentricity $\lambda = 0.5$

In Fig. 4 is shown the comparison of dimensionless pressure distributions in the lubricating gap: a) in the cross section, and b) in the longitudinal section, at the point of maximum dimensionless pressure p_{1max}, for a bearing with dimensionless length $L_1 = 0.5$ and the relative eccentricity $\lambda = 0.9$.

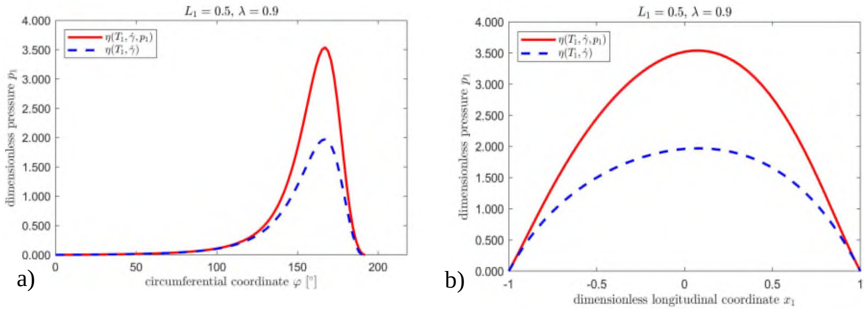

Fig. 4. The comparison of dimensionless pressure distributions p_1 in the lubricating gap: a) cross section, b) longitudinal section, at the point of maximum dimensionless pressure p_{1max}, for a bearing with dimensionless length $L_1 = 0.5$ and the relative eccentricity $\lambda = 0.9$

The comparisons of the calculated pressure distributions show, that taking into account the influence of pressure on the viscosity of the lubricating oil becomes more important for the cases, where the pressure generated in the lubricating gap is greater. In Fig. 5 is shown the comparison of: a) maximum dimensionless pressure p_{1max}, b) mean dimensionless pressure p_{1a} in the lubrication of the bearing with dimensionless length: $L_1 = 0.5$, depending on the relative eccentricity λ.

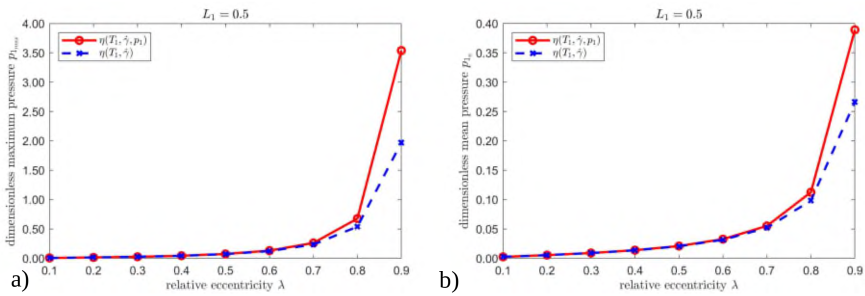

Fig. 5. The comparison of: a) maximum dimensionless pressure p_{1max}, b) mean dimensionless pressure p_{1a}, in the lubrication gap of the bearing with dimensionless length: $L_1 = 0.5$, for the considered relative eccentricities λ

The effect of taking into account pressure changes on the viscosity of the lubricating oil becomes noticeable at relative eccentricities of $\lambda = 0.7$ and greater. The same nature of the curves and the differences between them can be observed in the case of the transverse C_{1T} and the longitudinal C_{1L} dimensionless components of the bearing load carrying capacity, presented in Fig. 6.

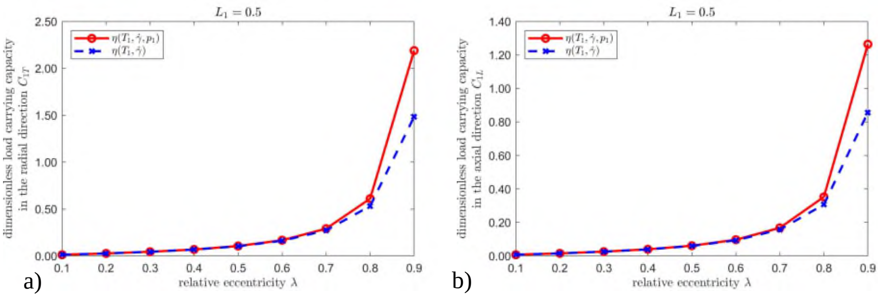

Fig. 6. The comparison of: a) transverse C_{1T}, b) longitudinal C_{1L} dimensionless components of the bearing load carrying capacity, of the bearing with dimensionless length: $L_1 = 0.5$, for the considered relative eccentricities λ

Figure 7a shows the calculated values of dimensionless friction force Fr_1, while in Fig. 7b are shown the values of friction coefficient μ_r, defined by Eq. (35).

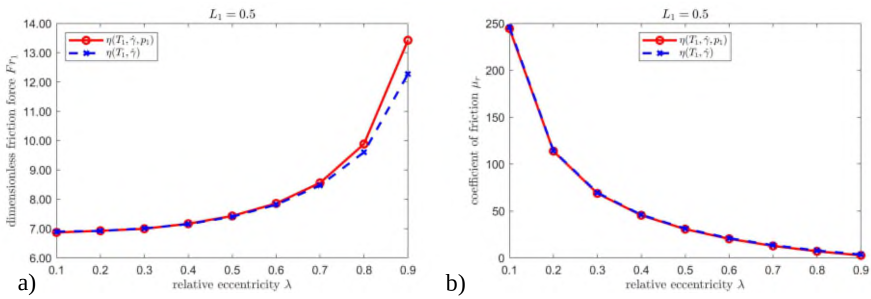

Fig. 7. The comparison of the calculated: a) friction force Fr_1, b) friction coefficient μ_r of the bearing with dimensionless length: $L_1 = 0.5$ and the considered relative eccentricities λ

The results for the bearing with dimensionless length $L_1 = 0.5$ show, that taking into account the influence of pressure on the viscosity of the lubricating oil is important for large relative eccentricities, i.e. $\lambda = 0.7$ and greater, which can be considered as extreme values of the relative eccentricities of the hydrodynamic bearing operation. The differences in the values of the friction coefficient in the adopted scale are irrelevant, however, they will even reach 26%, which will be shown later in this paper.

In Fig. 8 is shown the comparison of: a) maximum dimensionless pressure p_{1max}, b) mean dimensionless pressure p_{1a} in the lubrication of the bearing with dimensionless length: $L_1 = 1.0$, depending on the relative eccentricity λ.

The transverse C_{1T} and the longitudinal C_{1L} dimensionless components of the bearing load carrying capacity of the bearing with dimensionless length: $L_1 = 1.0$, depending on the relative eccentricity λ, are presented in Fig. 9, while Fig. 10 shows the calculated values of dimensionless friction force Fr_1 and the values of friction coefficient.

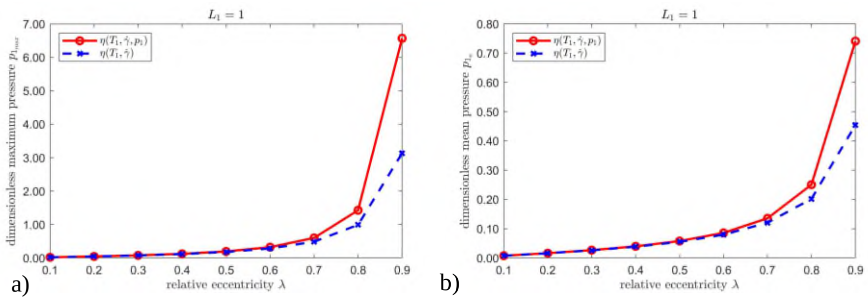

Fig. 8. The comparison of: a) maximum dimensionless pressure p_{1max}, b) mean dimensionless pressure p_{1a}, in the lubrication gap of the bearing with dimensionless length: $L_1 = 1.0$, for the considered relative eccentricities λ

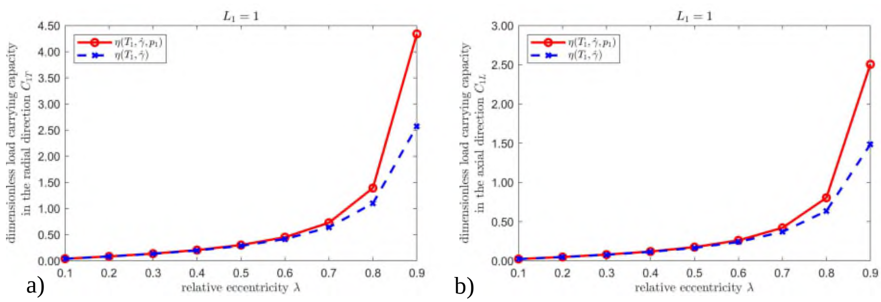

Fig. 9. The comparison of: a) transverse C_{1T}, b) longitudinal C_{1L} dimensionless components of the bearing load carrying capacity, of the bearing with dimensionless length: $L_1 = 1.0$, for the considered relative eccentricities λ

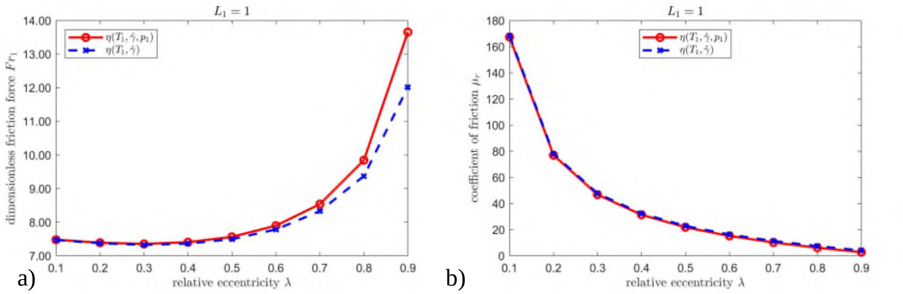

Fig. 10. The comparison of the calculated: a) friction force Fr_1, b) friction coefficient μ_r, for bearing with dimensionless length: $L_1 = 1.0$, and for the considered relative eccentricities λ

In the case of a bearing with dimensionless length $L_1 = 1.0$, higher values of dimensionless pressure, generated in the lubrication gap, are observed, than for a bearing with dimensionless length $L_1 = 0.5$, therefore taking into account the influence of pressure on the viscosity of the lubricating oil becomes more significant and is already noticeable at $\lambda = 0.6$ or even $\lambda = 0.5$, which corresponds to the values of relative eccentricities more similar to those found in practice under normal operating conditions of slide bearings.

Tab. 1 shows the relative changes of the calculated values, where the value obtained when considering the influence of pressure on the viscosity of the lubricating oil has been compared to the value when the influence of pressure on viscosity was neglected, according to the formula:

$$\delta X = \frac{\left(X_{T_1,\dot{\gamma},p_1} - X_{T_1,\dot{\gamma}}\right)}{X_{T_1,\dot{\gamma}}} \cdot 100\,\% \;, \tag{36}$$

where:

- δX [%] – calculated relative change in value,
- $X_{T_1,\dot{\gamma},p_1}$ – the considered value if the influence of pressure on viscosity of the lubricating oil is taken into account,
- $X_{T_1,\dot{\gamma}}$ – the considered value when the influence of pressure on viscosity of the lubricating oil is neglected.

The relative changes in the values shown in the Tab. 1 are for the bearings with dimensionless lengths of: $L_1 = 0.5$, $L_1 = 1.0$ and $L_1 = 1.5$. The minus sign signifies a decrease in the considered value $X_{T_1,\dot{\gamma},p_1}$, in relation to the reference value $X_{T_1,\dot{\gamma}}$.

Table 1

The relative changes of the calculated values (calculated according to Eq. (36))

L_1 [1]	λ [1]	δp_{1max} [%]	δp_{1a} [%]	δC_{1T} [%]	δC_{1L} [%]	δFr_1 [%]	$\delta \mu_r$ [%]
0.5	0.1	0.3	0.7	0.2	0.2	-0.4	-0.6
	0.2	0.7	0.4	0.5	0.5	0.1	-0.4
	0.3	1.3	1.3	0.9	0.9	-0.2	-1.0
	0.4	2.1	1.2	1.3	1.3	0.2	-1.1
	0.5	3.5	1.9	2.1	2.1	0.3	-1.8
	0.6	6.0	3.3	3.6	3.6	0.5	-2.9
	0.7	11.3	6.1	6.6	6.6	1.0	-5.2
	0.8	25.4	14.5	14.8	14.8	2.9	-10.4
	0.9	79.6	46.1	47.6	47.6	9.4	-25.9
1.0	0.1	1.0	0.6	0.7	0.7	0.1	-0.6
	0.2	2.2	1.3	1.5	1.5	0.2	-1.2
	0.3	3.7	2.2	2.4	2.4	0.4	-2.0
	0.4	5.7	3.3	3.7	3.7	0.6	-3.0
	0.5	8.7	5.0	5.5	5.5	0.9	-4.4
	0.6	13.6	7.6	8.5	8.5	1.4	-6.5
	0.7	23.0	12.6	14.0	14.0	2.5	-10.1
	0.8	44.1	24.0	26.6	26.6	5.0	-17.0
	0.9	109.7	63.1	68.8	68.8	13.6	-32.7
1.5	0.1	1.6	0.9	1.1	1.1	0.1	-0.9
	0.2	3.4	2.0	2.3	2.3	0.3	-1.9
	0.3	5.6	3.3	3.8	3.8	0.6	-3.1
	0.4	8.5	4.9	5.6	5.6	0.9	-4.4
	0.5	12.6	7.1	8.1	8.1	1.4	-6.2
	0.6	18.7	10.0	11.6	11.6	1.4	-9.1
	0.7	30.9	16.7	19.0	19.0	3.6	-12.9
	0.8	56.6	30.2	34.5	34.5	7.0	-20.5
	0.9	125.7	74.0	82.7	82.7	17.8	-35.5

For the greater dimensionless bearing lengths and greater values of relative eccentricity, the greater values of dimensionless pressure in the lubricating gap are obtained, therefore taking into account the influence of pressure on the viscosity of the lubricating oil is more important. The relative changes in the transverse and longitudinal components of bearing load carrying capacity, of course, are the same in each case, thus the relative changes of the resultant load carrying capacity will be equal to them. For a bearing with a dimensionless length of $L_1 = 1.5$, already at $\lambda = 0.5$, the relative changes of components of bearing load carrying capacity values exceed 8%.

Taking into account the influence of pressure on the viscosity of the lubricating oil causes relative increases in the calculated values of the bearing load carrying capacities, which are greater than the relative increases in the values of the friction force, hence there is a reduction of the calculated values of the friction coefficient.

4. Summary

The results presented in the paper show, that in some cases, taking into account the influence of pressure on the viscosity of the lubricating oil is crucial in modeling of the hydrodynamic lubrication of a conical slide bearing, and this is all the more important, the higher are the values of the dimensionless pressure generated in the bearing lubrication gap. The greater the dimensionless length of the bearing and the greater the relative eccentricity, the higher the dimensionless pressures in the lubricating gap, so considering the effect of pressure on viscosity also gives greater relative changes.

In this research it was assumed that the considered oil properties, in particular, its viscosity and its dependence on temperature, shear rate and pressure, are the same as the properties of 2% ferro-oil presented in paper [4]. This ferro-oil is characterized by quite high viscosity values compared to other, more popular engine oils, therefore in this work the influence of taking into account the dependence of oil viscosity on pressure in the simulations could be clearly visible, thus, the research will be continued in order to verify and evaluate the impact of taking into account changes in oil viscosity as a function of pressure, for classic oils with relatively lower viscosity values, on conical bearing hydrodynamic lubrication simulations results. Moreover, new models will be searched for determining changes in oil viscosity as a function of pressure.

The adopted hydrodynamic lubrication model can be used for the steady state lubrication of the conical slide bearings, when a constant temperature and heat flux at bearing shaft surface are known. Particular difficulties in modeling may be caused by the unknown value or distribution of the heat flux transferred from the oil in the lubricating gap to the inner surface of the shell. In the paper [2] was shown the influence of the value of heat flux at the inner surface of the shell, on the results obtained with this model. In these considerations it has been assumed that $q_{c1} = 0$, which would mean that the heat generated in the lubrication gap due to viscous heating does not flows out thorough the shell. In general, it can be expected that the heat flows through the shell from the lubrication gap, so the temperature of the oil is actually slightly lower, thus taking into account the influence of pressure on the viscosity of the oil in this case would be even more significant. Of course, the greater viscosity causes the more heat generation in the lubricating oil, thereby reducing its viscosity, thus reducing the viscous heating again. It is difficult to determine the final effect and values of the flow and operating parameters in such a case, without further testing, therefore such considerations are also the purpose of subsequent works.

The main conclusions of this research are as follows:

- pressure, as well as temperature and shear rate, affects the viscosity of the lubricating oil, therefore taking into account the effect of pressure may be important in modeling the hydrodynamic lubrication of slide bearings,
- the greater the dimensionless pressures generated in the lubricating gap, the more important it is to take into account the influence of the pressure on the viscosity of the lubricating oil,

- with relatively low dimensionless bearing lengths, taking into account the influence of pressure on viscosity is crucial at extremely high values of relative eccentricity, for greater dimensionless bearing lengths, this influence is significant already at smaller, more similar to the actual values of relative eccentricity, at which the bearings usually operate.

In this work, the use of analytical solutions of simplified equations of momentum and energy causes, that, there is no need to numerically solve systems of equations, in order to determine the components of velocity vector and temperature values. This significantly reduced the computer memory usage and the calculation time, because due to the fact that the mesh had 100 elements in the direction of the wrap angle and 50 in the direction of the bearing length, a matrix with [100x50]x[100x50] elements was created and inverted in the calculations in each calculation step. The lubricating gap was also divided into 10 elements in the direction of its height, but in this case the values of temperature, the components of oil velocity vector and shear rate were determined using the analytical solutions.

5. References

1. Czaban, A., Analiza hydrodynamicznego smarowania ferroolejami stożkowego łożyska ślizgowego, PhD thesis, Gdynia Maritime University, Gdynia, 2019.
2. Czaban, A., Miszczak, A., Simulations of the influence of the heat flux at the shaft surface of the conical slide bearing on its hydrodynamic lubrication and operating parameters, Journal of KONES, Vol. 26, No. 4, Warszawa, 2019, pp. 29 – 37.
3. Flores, P., Ambrósio, J., Claro, J.C., Lankarani, H., Koshy, C., Lubricated revolute joints in rigid multibody systems, Nonlinear Dynamics, 56, 2009, pp. 277-295.
4. Frycz, M., Wpływ stężenia cząstek magnetycznych w ferro-oleju na parametry przepływowe i eksploatacyjne poprzecznych łożysk ślizg., PhD thesis, Gdynia Maritime University, Gdynia, 2018.
5. Gohar, R., Elastohydrodynamics, Imperial College Press, Singapore, 2001.
6. Kelley, C. T., Iterative Solution of Systems of Linear and Nonlinear Equations, Philadelphia, Society for Industrial i Applied Mathematics, 1995.
7. Miszczak, A., Analiza hydrodynamicznego smarowania ferrocieczą poprzecznych łożysk ślizgowych, Fundacja Rozwoju Akademii Morskiej, Gdynia, 2006.
8. Miszczak, A., Analiza hydrodynamicznego smarowania łożysk ślizgowych cieczami o właściwościach nienewtonowskich, Wydawnictwo Naukowe Instytutu Technologii Eksploatacji – PIB, Gdynia, Radom, 2019.
9. Schramm, G., Reologia. Podstawy i zastosowania, Ośrodek Wydawnictw Naukowych, Poznań, 1998.
10. Wierzcholski, K., Miszczak, A., Mathematical principles and methods of biological surface lubrication with phospholipids bilayers, Biosystems, Vol. 178, 2019, pp. 32 – 40.